

pubs.acs.org/journal/abseba Article

Micropatterned Silk-Fibroin/Eumelanin Composite Films for Bioelectronic Applications

Yun Hee Youn, Sayantan Pradhan, Lucília P. da Silva, Il Keun Kwon, Subhas C. Kundu, Rui L. Reis, Vamsi K. Yadavalli,* and Vitor M. Correlo*



Cite This: https://doi.org/10.1021/acsbiomaterials.1c00216



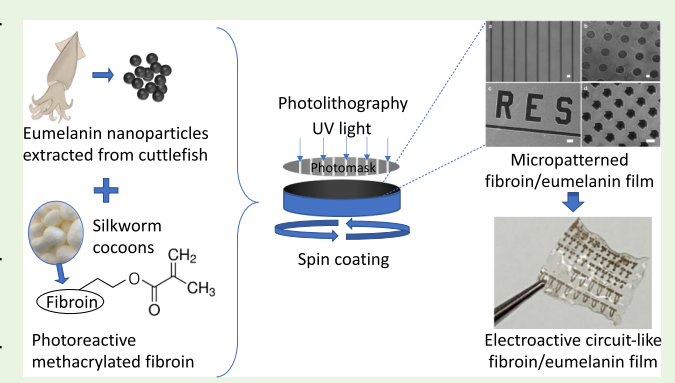
ACCESS

III Metrics & More

Article Recommendations

Supporting Information

ABSTRACT: There has been growing interest in the use of natural bionanomaterials and nanostructured systems for diverse biomedical applications. Such materials can confer unique functional properties as well as address concerns pertaining to sustainability in production. In this work, we propose the biofabrication of micropatterned silk fibroin/eumelanin composite thin films to be used in electroactive and bioactive applications in bioelectronics and biomedical engineering. Eumelanin is the most common form of melanin, naturally derived from the ink of cuttlefish, having antioxidant and electroactive properties. Another natural biomaterial, the protein silk fibroin, is modified with photoreactive chemical groups, which allows the formation of electroactive eumelanin thin films with different microstructures.



The silk fibroin/eumelanin composites are fabricated to obtain thin films as well as electroactive microstructures using UV curing. Here, we report for the first time the preparation, characterization, and physical, electrochemical, and biological properties of these natural silk fibroin/eumelanin composite films. Higher concentrations of eumelanin incorporated into the films exhibit a higher charge storage capacity and good electroactivity even after 100 redox cycles. In addition, the microscale structure and the cellular activity of the fibroin/eumelanin films are assessed for understanding of the biological properties of the composite. The developed micropatterned fibroin/eumelanin films can be applied as natural electroactive substrates for bioapplications (e.g., bioelectronics, sensing, and theranostics) because of their biocompatible properties.

KEYWORDS: silk fibroin, eumelanin, micropatterned thin films, electroactive properties, cellular activities

1. INTRODUCTION

Electroactive biomaterials have potential for impact in tissue engineering and biomedical applications owing to their capability of delivering electrical signals to trigger cellular activities. 1-3 The action potential of cell membranes is regulated by electric currents ranging from - 90 to +30 mV.4,5 Specific organs, such as the brain, skeletal muscle, and heart, are well known for their electrically sensitive properties, which incur either proliferation or differentiation of neuronal cells, myoblasts, and cardiomyocytes, respectively.⁶ Nevertheless, most of the researched electroactive biomaterials have been limited to synthetic conducting polymers, for example, poly[3,4-(ethylenedioxy)thiophene], polypyrrole, and polyaniline.⁵ Recently, naturally derived electroactive biomaterials have been increasingly sought as alternatives to synthetic polymers in tissue engineering and regenerative medicine. This is mainly because several naturally derived biopolymers, as well as their degradation byproducts, are less likely to be immunogenic.'

Melanin is a pigment synthesized by melanocytes of animals, microorganisms, and plants or by using chemical processes in

the laboratory. ^{10,11} It exists in different forms, pheomelanin or eumelanin, determining the color of the pigment—yellow to red (pheomelanin) or brown to black (eumelanin). Among the different forms, eumelanin is the most common type of melanin, naturally found in dark hair or cuttlefish ink, among others. ¹² Natural melanin nanoparticles and synthetic melanin-like nanomaterials have been suggested for biomedical applications because of their ultraviolet protection, radical scavenging, photothermal conversion, and biocompatibility. ^{13–15} Their intrinsic and unique electroactive properties have motivated their exploration as amorphous semiconductors ¹⁶ providing use in sensing, imaging, and therapeutics. ^{17–19} Among the kinds of naturally or artificially derived melanin nanoparticles, natural eumelanin nanoparticles extracted from

Received: February 10, 2021 Accepted: April 1, 2021



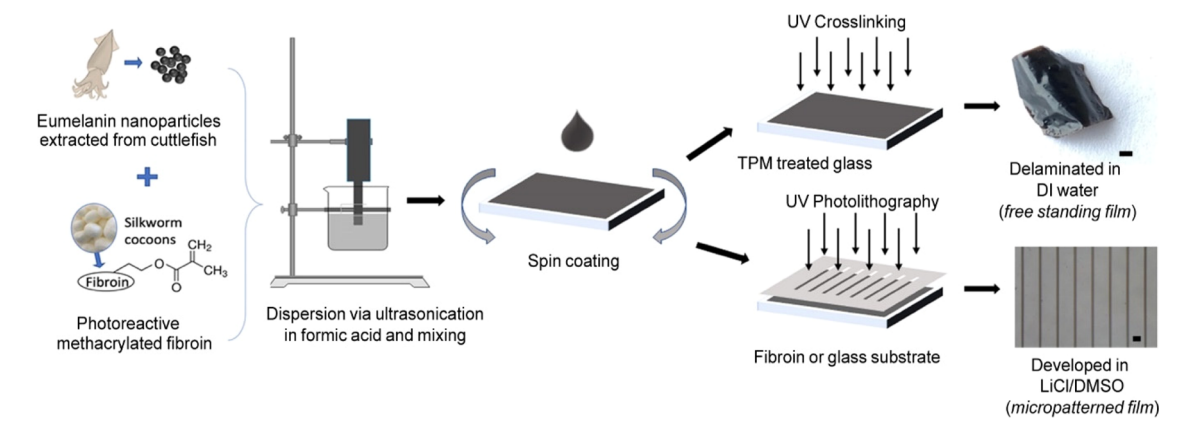


Figure 1. Schematic illustration of the process for silk fibroin/eumelanin composite formation and fabrication of cross-linked and micropatterned fibroin/eumelanin films. Spin coating was used to form free-standing films of cross-linked silk fibroin/eumelanin, shown here with 28% eumelanin to fibroin w/w (scale bar = 2 mm). Films are mechanically robust and flexible. Photolithography was used to fabricate the micropatterned alignments of fibroin/eumelanin film (scale bar = $100 \mu m$).

Sepia ink (*Sepia officinalis*) have attracted further interest owing to their inherent biosafety. ^{20,21} In addition, their antioxidant and electroactive properties have enabled eumelanin to be used for cardiac and skeletal muscle, neural tissue, or even bone tissue engineering applications. ^{22–25} The combination of nanomaterials with microtechnologies to be used in biomedical application has been emphasized. ^{26–28} In this context, the creation of macroscopic materials using eumelanin nanoparticles with tunable electro-optical properties is proposed by blending with a natural (structural) polymer.

Silk fibroin is a major component protein of silkworm silk extracted by a degumming process wherein the sticky glue protein of the cocoon, namely, sericin is removed.^{29,30} Silk fibroin from wild silkworm species contains the arginineglycine-aspartic acid (RGD) sequences, which are well known for cell attachment. 31,32 Conversely, silk fibroin from Bombyx. mori silkworms does not contain RGD sequences. Importantly, silk fibroin does not induce immunogenicity inside the body³ and has a slow biodegradation rate in vivo. 33,34 Therefore, silk fibroin-based biomaterials have been developed in the form of hydrogels, films, or fibers and explored as tissue engineering scaffolds in terms of cell proliferation, biofilm formation, pH-responsive and tunable permeability, and biosensing. 31,35,36 In recent studies, photolithography was reported to fabricate microstructured films using a silk fibroin modified with photoreactive acrylate groups.^{37,38} This has the potential to form precise patterns and architectures, 39 which can provide nano or microtopography for modulating cell behavior or bioelectronic circuits. ^{37,40} In this work, we fabricated phototunable silk fibroin films incorporating monodispersed, highdensity eumelanin nanoparticles, as well as electroactive microstructures via photolithography. The silk fibroin further provides a support matrix for the physical and electrical properties of eumelanin. We investigate the electrochemical properties and cellular metabolic activities of the mechanically robust, flexible, patterned composite films of silk fibroin incorporating eumelanin nanoparticles. These electroactive composite-based biomaterials have potential for various different types of tissue engineering, bioelectronics, and regenerative medicine applications.

2. MATERIALS AND METHODS

2.1. Extraction of Eumelanin Nanoparticles from the Ink Sacs of S. officinalis. Eumelanin was obtained from the ink sacs of

common cuttlefish (*S. officinalis*), as previously reported.²⁰ The ink was removed from the sacs, washed with distilled water, stirred in 6 N HCl (VWR, Belgium) for 24 h, and then centrifuged at 10,000 rpm for 15 min. The supernatant was discarded, and a second wash in 1 N HCl, water, and acetone was performed to eliminate any residues. The black pellet was collected and was dispersed in ultrapure water before the freeze-drying process.

2.2. Synthesis of Photoreactive Fibroin Protein. The silk protein fibroin (from *B. mori* silkworm cocoons, Mulberry Farms, USA) was converted into a photoactive form, named photofibroin, using a previously developed method.³⁷ Briefly, pure fibroin was dissolved in 1 M LiCl/DMSO and reacted with 2-isocyanatoethyl methacrylate in stoichiometric amounts for 5 h at 60 °C, while maintaining inert conditions using a constant flow of nitrogen. The reaction mixture was added to cold ethanol, and the methacrylated fibroin protein was obtained as the precipitate. The product was washed using a 1:1 ratio of cold ethanol and acetone followed by centrifugation and lyophilization. Chemical and nanoscale characterization of this material was earlier reported in detail.³⁷

2.3. Tensile Test. Samples were prepared by affixing films on an MTS 300 series tensile testing machine (MTS Systems Corporation, Eden Prairie, MN) equipped with a 50 N load cell. Measurements were taken at a strain rate of 0.1 mm/s, and data were collected at a rate of 10 Hz. Samples were 50 μ m thick as studied in this work.

2.4. Fabrication of Nonpatterned Fibroin/Eumelanin Films. *2.4.1. Preparation of a Fibroin/Eumelanin Composite Solution.* A composite solution composed of silk fibroin and eumelanin was prepared. Dry eumelanin powder (obtained from cuttlefish) was dispersed in formic acid (FA) (Acros Organics, 98%) by ultrasonicating the mixture for 40 min, resulting in a 1% (w/v) dispersion of eumelanin in FA. Photofibroin was mixed with the eumelanin dispersion to form a composite solution (Figure 1). The films contain only two components, that is, eumelanin and photofibroin because the solvent FA evaporates. Hence, the concentration of photofibroin is (100-concentration of eumelanin) %. Varying compositions with 12, 20, and 28% (w/w) eumelanin blended with photofibroin were studied. A photoinitiator (2-hydroxy-4'-(2-hydroxyethoxy)-2-methyl-propiophenone, Sigma-Aldrich) (2.5% (w/v) in the solution) was added to the composite before use.

2.4.2. Fabrication of Fibroin/Eumelanin Films. Films were fabricated by casting the composite solution of eumelanin and photofibroin (12, 20, and 28% (w/w) eumelanin) with appropriate amounts of photoinitiator, on clean glass slides (up to 1×1 inch). The glass slides were cleaned thoroughly using deionized (DI) water and ethanol prior to casting of the conductive prehydrogel composite solution. The hydrogel was left to dry under ambient conditions (21 $^{\circ}$ C) for 30 min and cross-linked under a 365 nm UV lamp (Lumen Dynamics OmniCure 1000 system) for 3 s at 20 mW cm⁻¹. The films

were immersed in DI water for 24 h to delaminate the films from the glass slides and to wash off the excess photoinitiator.

2.5. Fabrication of Fibroin/Eumelanin Composite Patterns. 2.5.1. Functionalization of Indium Tin Oxide (ITO)/Glass Slides. ITO-coated glass slides (Delta Technologies, Loveland, CO) and plain glass slides were first washed thoroughly with DI water and pure ethanol. The washed ITO slides were further cleaned using RCA cleaning solution (20:4:1 of $\rm H_2O/H_2O_2/NH_4OH$). The plain glass slides were cleaned using piranha solution (3:1 of $\rm H_2SO_4/H_2O_2$). Then, the ITO and plain glass slide surfaces were functionalized with 3-(trichlorosilyl) propyl methacrylate (TPM, Sigma-Aldrich) by chemical vapor deposition in a desiccator for 12 h at 0.4 bar (100 μ L of TPM) to obtain a self-assembled monolayer with pendant acrylate groups on the surface. These groups form covalent bonds with the methacrylate moieties present in the photofibroin when exposed under UV light, thus chemically cross-linking the fibroin/eumelanin composite to the ITO/glass slide surface.

2.5.2. Biofabrication of Composite Patterns. Micropatterns of the fibroin/eumelanin composite were fabricated on TPM-treated glass slides. The composite solution, 40 μ L of 1% eumelanin dispersion in FA and 3 mg of photofibroin, was spin-coated on the treated glass slide (1000 rpm for 40 s) to obtain a thin layer. The layer was airdried for a few seconds before exposing it under 365 nm UV light for 1 s through a photomask. The patterns were developed in 1 M LiCl/DMSO solution for 10 min followed by rigorous cleaning with DI water. The design and complexity of the patterns were defined by the design of the photolithographic mask. Patterns were fabricated on TPM-treated ITO slides using the same procedure.

2.6. Scanning Electron Microscopy (SEM) Imaging. SEM images of the fibroin/eumelanin composite patterned on TPM-treated glass slides were obtained using a Hitachi SU-field emission-scanning electron microscope to show the fidelity of the patterned structures. The patterns were sputter-coated in a 20 Å platinum Denton vacuum cold sputtering system (Moorestown NJ). Optical images were recorded using a Nikon Eclipse microscope. The morphologies of the dry fibroin/eumelanin patterns were also investigated using a high-resolution field emission scanning electron microscope with a focused ion beam (AURIGA COMPACT, ZEISS). Before analysis, the samples were sputtered with 1 nm of platinum. Samples were analyzed with an acceleration voltage of 3 kV, and different magnifications up to 5000× were used.

2.7. Atomic Force Microscopy (AFM). AFM was performed on the dry fibroin/eumelanin composite patterned on TPM-treated glass slides using an AFM Dimension Icon (Bruker, USA), operating in PeakForce Tapping (ScanAsyst) in air. AFM cantilevers (ScanAsyst-Air, Bruker) made of silicon nitride with a spring constant of 0.4 N/m and a frequency of 70 kHz were used. The AFM surface images were analyzed with NanoScope Analysis software (version 1.5).

2.8. Electrochemical Characterization. Cyclic voltammetry (CV) and linear sweep voltammetry (LSV) were performed on the fibroin/eumelanin electrodes with different eumelanin concentrations, fabricated on TPM-treated glass slides. PBS buffer (0.1 M and 7.4 pH) was used as the electrolyte. A standard three-cell setup uses Ag/ AgCl and Pt electrodes as reference and counter electrodes, respectively, while the fibroin/eumelanin composite on TPM-treated glass slides was used as the working electrode. CV and LSV were carried out on the samples using a Gamry Interface 1010E Potentiostat (Gamry Instruments, Warminster, PA) at a scan rate of 100 mV/sec over a potential window of -1.0-1.6 V. The charge storage capacity (CSC) of the samples was obtained from the area under the CV using OriginPro (Origin Lab). The average CSC from three samples from each eumelanin concentration is reported. The impedance spectra of the electrodes were determined in a frequency range of 10^{-2} – 10^5 Hz with a 5 mV AC amplitude.

2.9. Cell Culture and Cytotoxicity Test. L929 mouse lung fibroblasts (from the European Collection of Cell Cultures) were used to perform a cytotoxicity test on fibroin/eumelanin composite films. L929 fibroblasts were cultured with low glucose Dulbecco's modified Eagle's medium (Sigma, USA), supplemented with 10% (v/v) fetal bovine serum (Gibco, Invitrogen) and 1% (v/v) antibiotic-

antimycotic solution (Gibco, Invitrogen), and incubated at 37 $^{\circ}$ C in a humidified tissue culture incubator with a 5% CO₂ atmosphere. Cells were seeded at a density of 80,000 cells/cm², 25,000 cells/96-well plate. After 24 h, eumelanin film extracts were added to the cell culture. After 72 h, cell morphology was observed using an inverted microscope (AxioVert A1 FL LED, Zeiss). The cell metabolic activity was evaluated through a colorimetric MTS assay (MTS reagent (3(4, 5-dimethylthiazol-2-yl)-2, 5-diphenyltetrazolium bromide, Sigma). The eumelanin film extracts were prepared by loading the films (6 cm²) containing 12, 20, and 28% eumelanin on 1 mL of fresh cell culture medium and exposing them to stirring (180 rpm) and temperature (37 $^{\circ}$ C) for 24 h. 10% dimethyl sulfoxide (DMSO) was used as the positive control of cytotoxicity while cells maintained under standard conditions acted as the negative control of cytotoxicity.

2.10. Statistical Analysis. GraphPad software was used to perform statistical analysis. Data were analyzed with the Shapiro—Wilk normality test and then with the Kruskal—Wallis test with Dunn's multiple comparison post-test or one-way analysis of variance (ANOVA) with Tukey's multiple comparison test. Results are presented as mean \pm standard deviation (SD), and the significance level between groups was set for *p < 0.05, **p < 0.01, and ***p < 0.001.

3. RESULTS AND DISCUSSION

3.1. Film Formation and Micropatterning Using the Fibroin/Eumelanin Composite. The ability to form

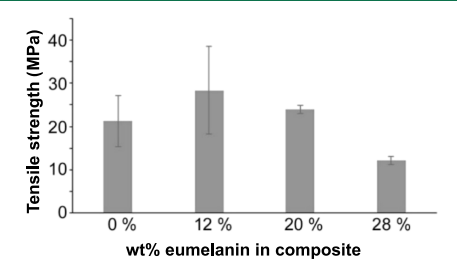


Figure 2. Tensile testing of the films of the fibroin/eumelanin biocomposite as a function of the % of eumelanin in the film (w/w). Note that the corresponding % of fibroin is 100-wt of eumelanin.

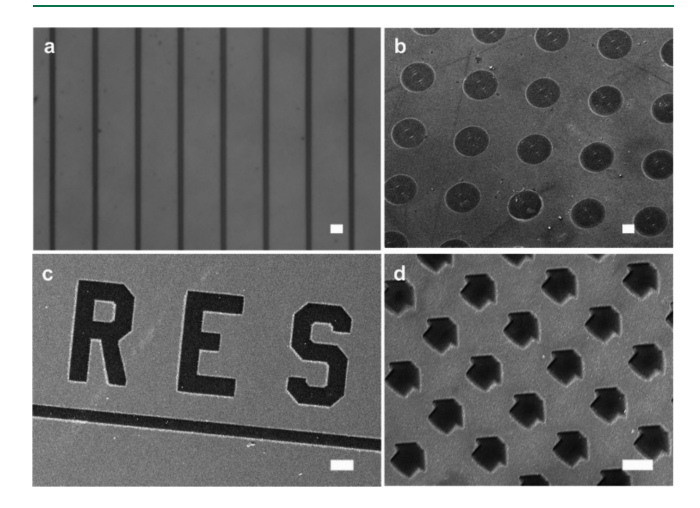


Figure 3. High-resolution micropatterning of the fibroin/eumelanin composite. The composite solution was spin-coated on a glass substrate to form various microscale patterns. Scale bar on all the panels = 100 μ m.

mechanically strong, flexible films and coatings, which are stable in physiological environments using eumelanin, is crucial for the realization of new electroactive applications. A number

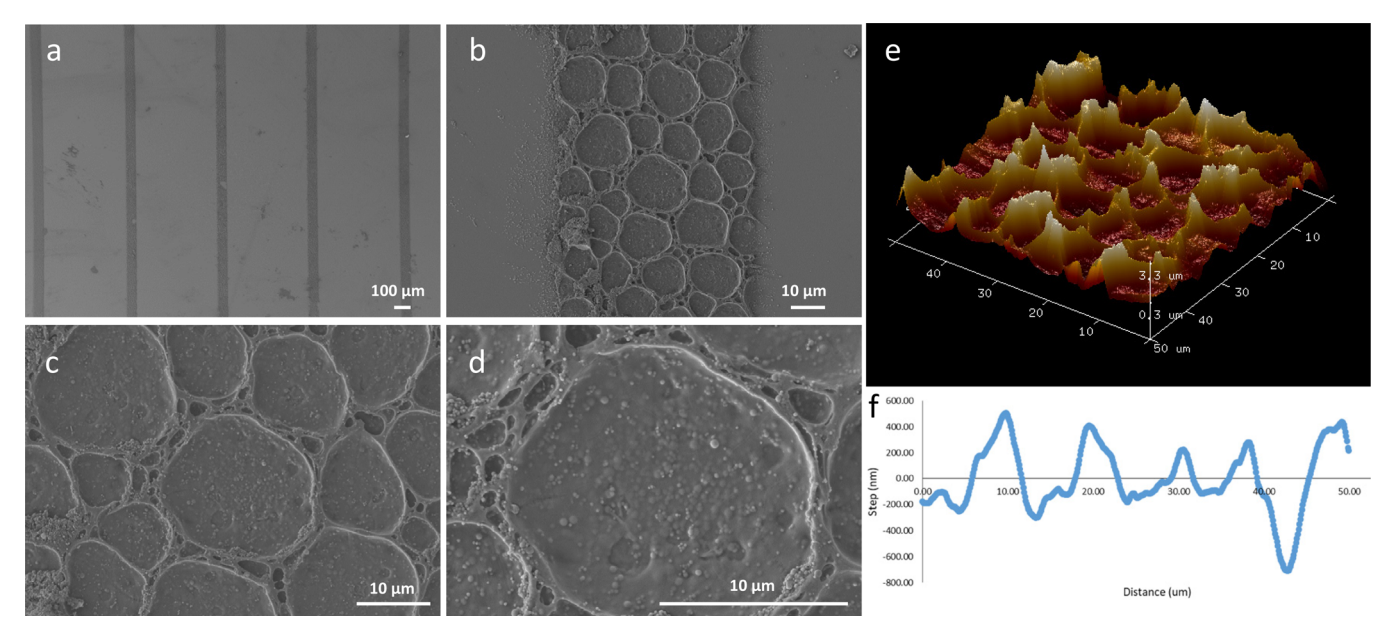


Figure 4. Physical properties of aligned micropatterns of the fibroin/eumelanin composite on glass slides were confirmed by SEM images (a–d) and AFM analysis (e, f). The composite solution was spin-coated on a glass substrate to form the micropatterns. Patterns of fibroin/eumelanin ranged from 50 to 60 μ m (a, magnification = 50×). A single micropattern was magnified $1000 \times$ (b). The various shapes at the microscale were formed by spin coating (c, magnification = 2500×). Eumelanin nanoparticles in the composite were observed at 5000 x of magnification (d). AFM image of the fibroin/eumelanin is measured with a scan size of 50 × 50 μ m (e) showing the step heights (f).

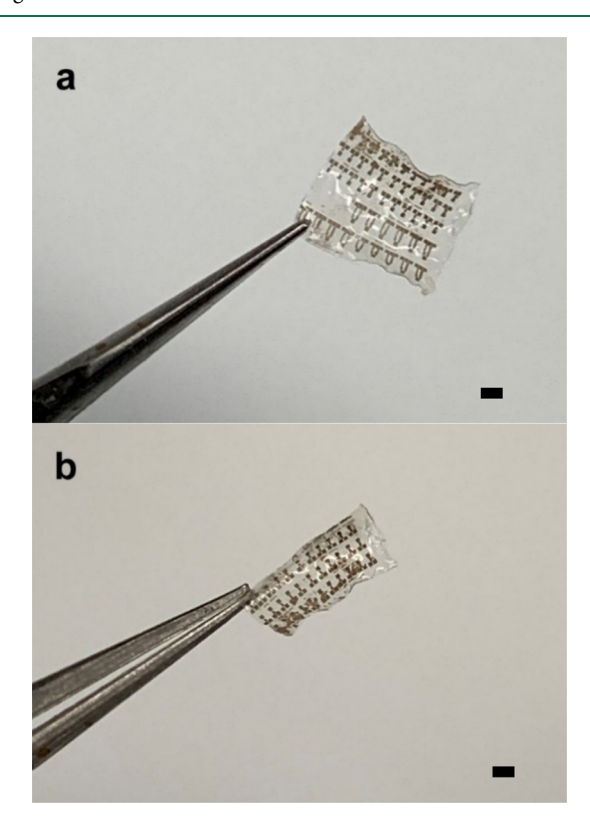


Figure 5. – High-resolution patterns of the fibroin/eumelanin composite can be printed on flexible fibroin sheets resulting in (a) micropatterned films that (b) can be rolled. Scale bar = 2 mm.

of strategies have been investigated over the years to obtain device-quality eumelanin films. Solution processing techniques using solvents such as DMSO, DMF, and aqueous ammonia have been reported to obtain smooth eumelanin films. ^{18,41–43} Free-standing eumelanin films have also been reported by the

electrochemical oxidation of aqueous L-dopa solutions. ⁴⁴ Eumelanin nanoparticles have been used in combination with natural polymers such as chitosan, carrageenan, and agar to obtain films with enhanced mechanical and biochemical properties. ^{45–47} Indeed, a composite of synthetic melanin and silk fibroin was reported for the fabrication of films, which was previously employed as a tissue engineering matrix. ²⁵ However, photopatternable composites of silk fibroin and natural eumelanin have not been reported to date. The ability to form photoreactive biocomposites of fibroin/eumelanin has the potential to form precisely controlled and patterned structures for electrically active tissue engineering.

A photoactive silk fibroin was previously used to realize mechanically robust films as well as form high-resolution micropatterns via a facile benchtop lithographic process. 37,48 In this work, the combination of eumelanin and the photofibroin is aimed at enhancing the versatility of patterns while rendering it compatible with photolithographic techniques. While eumelanins are insoluble in most organic solvents, which hinders their easy processing, 49 1% (w/v) dispersion of eumelanin could be obtained in FA by ultrasonication. Thus, a composite of the two materials could be formed, while varying their relative concentrations. For instance, eumelanin in the composite could be varied to almost 50% (w/w). This corresponds to 50% photofibroin (w/w) as the solvent evaporates during film formation. It may be noted that the FA does not affect the mechanical properties or photopatternability of the composite solution in the time taken to form the films. However, if left for a long period of time in solution (\sim 5 days), some discoloration in the solution is seen.

Free-standing films of varying thickness (typically $\sim 50~\mu m$, measured and crosschecked using SEM imaging, optical microscopy, and digital calipers) were formed by casting or spin-coating the photofibroin/eumelanin composite on clean glass slides followed by exposure to 365 nm UV light. The resulting free-standing films are easily detached from the

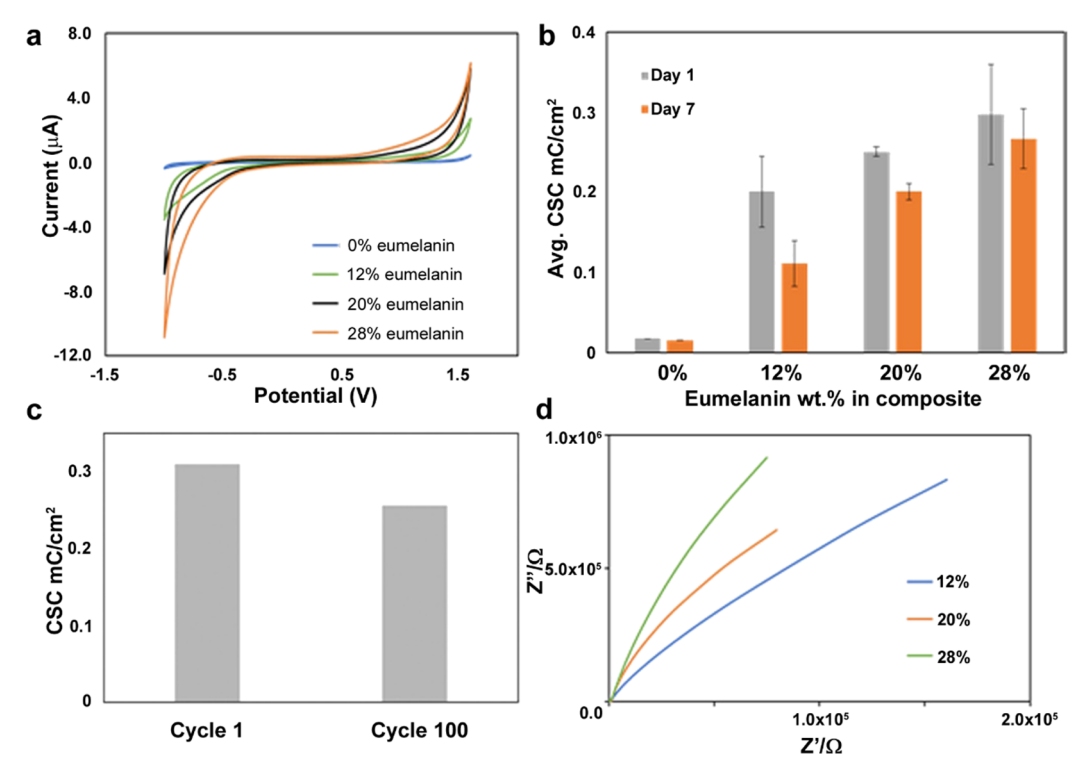


Figure 6. – Electrochemical characterization of the fibroin/eumelanin biocomposite on ITO substrates. (a) CV with varying % eumelanin (w/w) in composite, (b) CSC of the composite over 1 week, (c) effect of redox cycles on the electroactivity of the fibroin/eumelanin composite using 28% of eumelanin, and (d) Nyquist plots for the composite. PBS (0.1 M, 7.4 pH) was used as the electrolyte.

Table 1. Comparison of the Electrochemical Properties of the Eumelanin Composites Reported Earlier in the Literature

source of eumelanin	system	CV range (V)	scan rate (mV/s)	CSC	ref
synthetic	eumelanin on carbon paper	-0.4 to 0.4	5	$\frac{2.8}{\text{mC/cm}^2}$	63
synthetic	eumelanin on carbon paper	-0.35 to 0.3	5	24 mAh/g	62
natural	eumelanin+ AgNW	-0.7 to 0.3	1	49.3 mAh/g	67
natural	eumelanin-Na	-0.7 to 0.3		30.4 mAh/g	19

Table 2. Equivalent Circuit Model Fit of the EIS Data for Varying Compositions of the Fibroin/Eumelanin Composite

% eumelanin (w/w)	$R_{\rm s} \; (\Omega)$	$R_{\rm ct}~({ m M}\Omega)$	$CPE_{dl} (\mu F s^{a-1})$	$a_{ m dl}$
12%	234.3	108.00	3.27×10^{-6}	0.912
20%	153.9	46.98	3.34×10^{-6}	0.963
28%	254.6	23.05	1.41×10^{-6}	0.954

support on water immersion and are mechanically robust (Figure 1). Tensile testing on the films showed that the addition of eumelanin improves the strength of the fibroin films (12% eumelanin: 28.4 ± 10.2 MPa in comparison to 21.4 \pm 5.9 MPa for fibroin films without any eumelanin) (Figure 2). It may be noted that the values of tensile strength of regenerated silk fibroin (rSF) are in the same order of the values reported in the literature—a range of values has been reported from 4 to 30 MPa, depending on the preparation and measurement conditions. 50,51 This comparison is to show that

films formed by cross-linking are slightly stronger than rSF. However, the addition of more eumelanin causes the films to become weaker (28% eumelanin: 12.1 ± 1 MPa). Importantly, even at this concentration, the films are very robust and can easily be handled without breakage.

Patterns of fibroin/eumelanin on glass, ITO glass, or silicon substrates were fabricated via photolithography (Figure 3). The photoreactive fibroin in the composite behaves as a "negative photoresist," providing a stable and biocompatible matrix for entrapping the eumelanin. The fibroin/eumelanin composite solution was spin-coated on a TPM-functionalized surface and photocross-linked through a photomask to form microstructures. On exposure to UV light, the methacrylate moieties from photofibroin in the composite form covalent bonds with the pendant acrylate groups on the functionalized surface. This chemical conjugation anchors the patterns onto the substrate, thus forming high-fidelity structures that are stable in various solvents. Patterns were developed in 1 M LiCl/DMSO, whereby the un-cross-linked material dissolves in the developing solution.

The surface morphology of the aligned silk fibroin/eumelanin micropatterns (12% eumelanin) obtained by masking fabrication after spin coating was evaluated by SEM and AFM (Figure 4). The aligned micropatterns were fabricated in 50–60 μ m of diameter (Figure 4a). Moreover, the surface of the fibroin/eumelanin composites showed shapes at various microscales. The surfaces are typically smooth at the micro- and macroscales as seen in Figure 3 and the surface of the patterns (Figure S1). By observing the SEM image at 5000× (Figure 4d), the film presented a rough morphological structure made of aggregates of eumelanin nanoparticles. The shape of eumelanin was spherical at the nanoscale size. AFM was used to observe the nanoroughness of

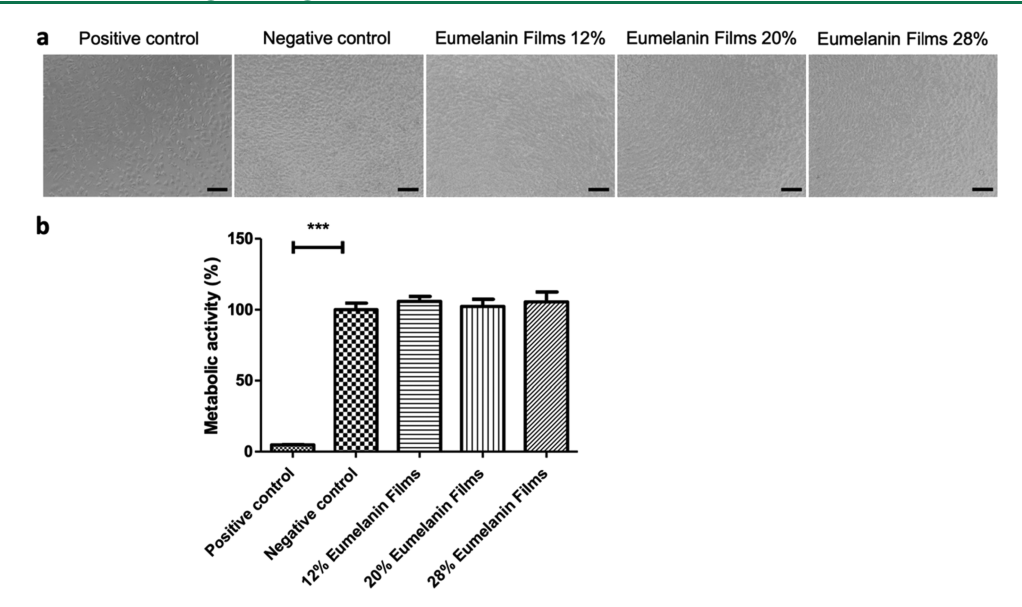


Figure 7. — Metabolic activity of L929 cells after 72 h of contact with fibroin/eumelanin film extracts. (a) L929 cell images were observed under the microscope (scale bar = $200 \, \mu \text{m}$). (b) Metabolic activity results show no cytotoxicity of fibroin/eumelanin films. Data are presented as mean \pm S.D. One way-ANOVA followed by Dunnett's multiple comparison test (in comparison to the negative control) was used to analyze data (*** p < 0.005).

the 12% eumelanin-containing fibroin films (Figure 4e). As fabricated on the slide glass by the spin coating method, the height of the well ranged from 400 to 800 nm (Figure 4f). The surface roughness of the fibroin/eumelanin composite was $R_{\rm a}$ = 633 nm and $R_{\rm q}$ = 819 nm, indicating that it might have been affected by eumelanin. Nanoroughness has been demonstrated to improve neural cell adhesion on the surface of substrates because of the increased contact area. Similarly, fibroin films with covalently attached fibroin/eumelanin patterns can be formed as seen in Figure 5. This implies that fibroin/eumelanin "circuits" can be formed on a variety of substrates including fibroin.

3.2. Electrochemical Characterization of the Silk Fibroin/Eumelanin Composite. Ever since the discovery of eumelanin as a naturally occurring amorphous semiconductor, there has been interest in eumelanin-based organic electronics, 16,53 Numerous studies have been reported for understanding the conduction mechanism of eumelanin along with its unique physical structure and photoprotective or antioxidant properties. ^{22,41,54–56} It is known that the hydration state of eumelanin has a significant effect on its electrical properties. 57,58 Various melanin-based devices, such as sensors, 59-61 energy storage devices, 19,62,63 and OECTs, 64 have been reported. Most electrochemical studies have been performed using melanin in ITO/glass and carbon paper or silicon as the substrate. Initially, fibroin/eumelanin electrodes were fabricated on functionalized ITO/glass. Electrochemical characterization of the composite at different compositions was performed using CV and electrochemical impedance spectroscopy (EIS).

A scan was performed over -1.0 to 1.6 V at a scan rate of 100 mV/s with varying eumelanin concentrations (Figure 6a). This range was selected as a standard wide potential window. The electroactivity and electrochemical stabilities of the eumelanin composites were characterized in terms of CSC. The electroactivity of the composite increases with an increase in the concentration of eumelanin (Figure 6b). The electrodes with a 28% eumelanin (w/w) composite showed a CSC of

 $\sim 0.3 \text{ mC/cm}^2$. This is comparable to the values reported in the literature, where the CSC value of pure eumelanin was found to be 1.8 to 2.8 mC/cm², which, in turn, is affected when formed in a composite with other materials (Table 1).⁶³ The stability of eumelanin on an ITO substrate is a major concern while performing electrochemical experiments. 62 The presence of fibroin in the composite chemically adhered the film onto the ITO surface, which prevented the film from delaminating. This increased the stability of the entire system. The 28% eumelanin incorporated into the fibroin composite was able to retain ~90% of its electroactivity even after 7 days of soaking in PBS. Furthermore, the material was able to retain ~83% of its electroactivity after 100 redox cycles (Figure 6c). Exemplary characteristics for conjugated polymers in applications such as neural interfaces have been previously covered in excellent reviews. As eumelanin itself has been shown in nerve tissue engineering, ^{18,50,65,66} these properties suggest that the fibroin/ eumelanin composite is a viable alternative to synthetic conjugated polymers for various applications in bioelectronics.

EIS spectra of varying eumelanin concentrations in silk fibroin/eumelanin composites were recorded. Figure 6d shows the Nyquist plots of three different electrode compositions. A simple Randles equivalent circuit with a parallel resistance and a constant phase element connected in series with a resistance was constructed. The values from the fitting are presented in Table 2. The resistance of the solution is almost the same in each case, which implies that the electrolyte imposes comparable resistance. There is no significant change in the double layer nonideal capacitance of the electrodes. There is a clear decrease in the charge transfer resistance from 108 to 23.05 M Ω upon increasing the concentration of the eumelanin in the composite (Table 2), which indicates that the electrochemical properties are modulated by the eumelanin. The Bode plots for the composite at different eumelanin concentrations (w/w) are provided in Figure S2 in the Supporting Information.

3.3. Cytotoxicity Screening of Silk Fibroin/Eumelanin Composite Extracts. The fibroin/eumelanin composite

extracts were tested for cytotoxicity on L929 murine fibroblasts. The morphology of the cells was not affected after 72 h of incubation with the extracts (Figure 7a). The cellular metabolic activity was also measured by the MTS assay (Figure 7b). Cells incubated with the extracts have shown good cell metabolic activity, which means that none of the samples were cytotoxic. A slightly higher cell viability was observed for fibroin/eumelanin composites compared to the standard condition as the negative control of cytotoxicity. This indicates that the biocomposite is biofriendly. From our results of cell activity, the fibroin/eumelanin composites can be considered as a promising biomaterial for tissue engineering and different applications in biomedical fields. From earlier work from our and other groups, the biodegradation of silk fibroin (both rSF and photofibroin) was shown via hydrolytic enzymatic action. Thus, composites of fibroin and eumelanin are also expected to be degradable, which raises prospects for their use in various regenerative medicine applications, where there has been concern because of the nondegradability of the electroactive component (e.g., nanocarbons, metals, conducting polymers, etc.).

4. CONCLUSIONS

In summary, we present a natural electroactive biocomposite formed from silk fibroin (structural component) and eumelanin (electroactive component). This fibroin/eumelanin composite can be formed into films using the simple technique of spin coating followed by UV cross-linking and also patterned into microstructures via photolithography. The mechanical properties and electroconductivity of the nanocomposite films were meaningfully enhanced with flexible strength and microscale morphology. The films had a roughness average size of 633 nm with CSC of ~0.3 mC/ cm². In addition, the biocomposite was also confirmed as a noncytotoxic material by cellular metabolic assessments. The natural fibroin/eumelanin composite films with improved mechanical properties and electroactivity could be used for active biomedical applications (e.g., biosensing, theranostics, and others).

ASSOCIATED CONTENT

Supporting Information

The Supporting Information is available free of charge at https://pubs.acs.org/doi/10.1021/acsbiomaterials.1c00216.

The SEM image of the pattern surface and the Bode plots of the composites (PDF)

■ AUTHOR INFORMATION

Corresponding Authors

Vamsi K. Yadavalli — Department of Chemical & Life Science Engineering, Virginia Commonwealth University, Richmond, Virginia 23284-3028, United States; orcid.org/0000-0002-8879-1948; Email: vyadavalli@vcu.edu

Vitor M. Correlo — 3B's Research Group, I3Bs — Research Institute on Biomaterials, Biodegradables and Biomimetics, University of Minho, Headquarters of the European Institute of Excellence on Tissue Engineering and Regenerative Medicine, Barco, Guimares 4805-017, Portugal; ICVS/3B's—PT Government Associate Laboratory, Braga, Guimaraes 4806-909, Portugal; Email: vitorcorrelo@i3bs.uminho.pt

Authors

Yun Hee Youn − 3B's Research Group, I3Bs − Research Institute on Biomaterials, Biodegradables and Biomimetics, University of Minho, Headquarters of the European Institute of Excellence on Tissue Engineering and Regenerative Medicine, Barco, Guimares 4805-017, Portugal; ICVS/3B's−PT Government Associate Laboratory, Braga, Guimaraes 4806-909, Portugal; Department of Dental Materials, School of Dentistry, Kyung Hee University, Seoul 02447, Republic of Korea; orcid.org/0000-0003-0544-3719

Sayantan Pradhan — Department of Chemical & Life Science Engineering, Virginia Commonwealth University, Richmond, Virginia 23284-3028, United States

Lucília P. da Silva — 3B's Research Group, I3Bs — Research Institute on Biomaterials, Biodegradables and Biomimetics, University of Minho, Headquarters of the European Institute of Excellence on Tissue Engineering and Regenerative Medicine, Barco, Guimares 4805-017, Portugal; ICVS/3B's—PT Government Associate Laboratory, Braga, Guimarães 4806-909, Portugal

Il Keun Kwon – Department of Dental Materials, School of Dentistry, Kyung Hee University, Seoul 02447, Republic of Korea: Ocid.org/0000-0001-9649-3003

Subhas C. Kundu — 3B's Research Group, I3Bs — Research Institute on Biomaterials, Biodegradables and Biomimetics, University of Minho, Headquarters of the European Institute of Excellence on Tissue Engineering and Regenerative Medicine, Barco, Guimares 4805-017, Portugal; ICVS/3B's—PT Government Associate Laboratory, Braga, Guimaraes 4806-909, Portugal

Rui L. Reis — 3B's Research Group, I3Bs — Research Institute on Biomaterials, Biodegradables and Biomimetics, University of Minho, Headquarters of the European Institute of Excellence on Tissue Engineering and Regenerative Medicine, Barco, Guimares 4805-017, Portugal; ICVS/3B's—PT Government Associate Laboratory, Braga, Guimaraes 4806-909, Portugal; Department of Dental Materials, School of Dentistry, Kyung Hee University, Seoul 02447, Republic of Korea

Complete contact information is available at: https://pubs.acs.org/10.1021/acsbiomaterials.1c00216

Notes

The authors declare no competing financial interest.

ACKNOWLEDGMENTS

The authors acknowledge the FRONTHERA project (Frontiers of technology for theranostics of cancer, metabolic and neurodegenerative diseases) n° NORTE-01-0145-FEDER-0000232, the European Union Framework Programme for Research and Innovation Horizon 2020 under grant agreement n° 668983 — FoReCaST (Forefront Research in 3D Disease Cancer Models as in vitro Screening Technologies), and FCT grants POCI-01-0145-FEDER-031590, PD/BD/150546/2019 and PTDC/BTM-ORG/28168/2017. VKY acknowledges support from the National Science Foundation (CBET-1704435).

REFERENCES

(1) Tandon, B.; Magaz, A.; Balint, R.; Blaker, J. J.; Cartmell, S. H. Electroactive Biomaterials: Vehicles for Controlled Delivery of

- Therapeutic Agents for Drug Delivery and Tissue Regeneration. *Adv. Drug Delivery Rev.* **2018**, *129*, 148–168.
- (2) Balint, R.; Cassidy, N. J.; Cartmell, S. H. Conductive Polymers: Towards a Smart Biomaterial for Tissue Engineering. *Acta Biomater.* **2014**, *10*, 2341–2353.
- (3) Guiseppi-Elie, A. Electroconductive Hydrogels: Synthesis, Characterization and Biomedical Applications. *Biomaterials* **2010**, 31, 2701–2716.
- (4) Lengyel, C.; Iost, N.; Virág, L.; Varró, A.; Lathrop, D. A.; Papp, J. G. Pharmacological Block of the Slow Component of the Outward Delayed Rectifier Current ($I_{\rm Ks}$) Fails to Lengthen Rabbit Ventricular Muscle QT $_{\rm c}$ and Action Potential Duration. *Br. J. Pharmacol.* **2001**, 132, 101–110.
- (5) Ning, C.; Zhou, Z.; Tan, G.; Zhu, Y.; Mao, C. Electroactive Polymers for Tissue Regeneration: Developments and Perspectives. *Prog. Polym. Sci.* **2018**, *81*, 144–162.
- (6) Kim, H. N.; Jiao, A.; Hwang, N. S.; Kim, M. S.; Kang, D. H.; Kim, D.-H.; Suh, K.-Y. Nanotopography-Guided Tissue Engineering and Regenerative Medicine. *Adv. Drug Delivery Rev.* **2013**, *65*, 536–558
- (7) Ullah, S.; Chen, X. Fabrication, Applications and Challenges of Natural Biomaterials in Tissue Engineering. *Appl. Mater. Today* **2020**, 20, No. 100656.
- (8) Shi, Z.; Gao, X.; Ullah, M. W.; Li, S.; Wang, Q.; Yang, G. Electroconductive Natural Polymer-Based Hydrogels. *Biomaterials* **2016**, *111*, 40–54.
- (9) Ramanavicius, S.; Ramanavicius, A. Conducting Polymers in the Design of Biosensors and Biofuel Cells. *Polymer* **2021**, *13*, 49.
- (10) Martínez, L. M.; Martinez, A.; Gosset, G. Production of Melanins With Recombinant Microorganisms. *Front. Bioeng. Biotechnol.* **2019**, 7, 285.
- (11) Haywood, R. M.; Lee, M.; Linge, C. Synthetic Melanin Is a Model for Soluble Natural Eumelanin in UVA-Photosensitised Superoxide Production. *J. Photochem. Photobiol. B* **2006**, 82, 224–235.
- (12) Solano, F. Melanins: Skin Pigments and Much More—Types, Structural Models, Biological Functions, and Formation Routes. *New J. Sci.* **2014**, *2014*, *1*–28.
- (13) Park, J.; Moon, H.; Hong, S. Recent Advances in Melanin-like Nanomaterials in Biomedical Applications: A Mini Review. *Biomater. Res.* **2019**, 23, 1–10.
- (14) Caldas, M.; Santos, A. C.; Veiga, F.; Rebelo, R.; Reis, R. L.; Correlo, V. M. Melanin Nanoparticles as a Promising Tool for Biomedical Applications a Review. *Acta Biomater.* **2020**, 26.
- (15) Wang, X.; Sheng, J.; Yang, M. Melanin-Based Nanoparticles in Biomedical Applications: From Molecular Imaging to Treatment of Diseases. *Chin. Chem. Lett.* **2019**, *30*, 533–540.
- (16) McGinness, J.; Corry, P.; Proctor, P. Amorphous Semi-conductor Switching in Melanins. *Science* **1974**, *183*, 853–855.
- (17) D'Ischia, M.; Napolitano, A.; Pezzella, A.; Meredith, P.; Sarna, T. Chemical and Structural Diversity in Eumelanins: Unexplored Bio-Optoelectronic Materials. *Angew. Chem., Int. Ed.* **2009**, *48*, 3914–3921.
- (18) Bettinger, C. J.; Bruggeman, P. P.; Misra, A.; Borenstein, J. T.; Langer, R. Biocompatibility of Biodegradable Semiconducting Melanin Films for Nerve Tissue Engineering. *Biomaterials* **2009**, *30*, 3050–3057.
- (19) Kim, Y. J.; Wu, W.; Chun, S.-E.; Whitacre, J. F.; Bettinger, C. J. Biologically Derived Melanin Electrodes in Aqueous Sodium-Ion Energy Storage Devices. *Proc. Natl. Acad. Sci.* **2013**, *110*, 20912–20917.
- (20) da Silva, L. P.; Oliveira, S.; Pirraco, R. P.; Santos, T. C.; Reis, R. L.; Marques, A. P.; Correlo, V. M. Eumelanin-Releasing Spongy-like Hydrogels for Skin Re-Epithelialization Purposes. *Biomed. Mater.* **2017**, *12*, No. 025010.
- (21) Srisuk, P.; Bishi, D. K.; Berti, F. V.; Silva, C. J. R.; Kwon, I. K.; Correlo, V. M.; Reis, R. L. Eumelanin Nanoparticle-Incorporated Polyvinyl Alcohol Nanofibrous Composite as an Electroconductive Scaffold for Skeletal Muscle Tissue Engineering. *ACS Appl. Bio Mater.* **2018**, *1*, 1893–1905.

- (22) Mostert, A. B.; Powell, B. J.; Pratt, F. L.; Hanson, G. R.; Sarna, T.; Gentle, I. R.; Meredith, P. Role of Semiconductivity and Ion Transport in the Electrical Conduction of Melanin. *Proc. Natl. Acad. Sci.* **2012**, *109*, 8943–8947.
- (23) Kim, E.; Liu, Y.; Leverage, W. T.; Yin, J.-J.; White, I. M.; Bentley, W. E.; Payne, G. F. Context-Dependent Redox Properties of Natural Phenolic Materials. *Biomacromolecules* **2014**, *15*, 1653–1662.
- (24) Nune, M.; Manchineella, S.; Govindaraju, T.; Narayan, K. S. Melanin Incorporated Electroactive and Antioxidant Silk Fibroin Nanofibrous Scaffolds for Nerve Tissue Engineering. *Mater. Sci. Eng.* C **2019**, *94*, 17–25.
- (25) Manchineella, S.; Thrivikraman, G.; Khanum, K. K.; Ramamurthy, P. C.; Basu, B.; Govindaraju, T. Pigmented Silk Nanofibrous Composite for Skeletal Muscle Tissue Engineering. *Adv. Healthcare Mater.* **2016**, *5*, 1222–1232.
- (26) Ung, T.; Liz-Marzán, L. M.; Mulvaney, P. Gold Nanoparticle Thin Films. *Colloids Surf. Physicochem. Eng. Asp.* **2002**, 202, 119–126.
- (27) Montiel-González, Z.; Rodil, S. E.; Muhl, S.; Mendoza-Galván, A.; Rodríguez-Fernández, L. Amorphous Carbon Gold Nanocomposite Thin Films: Structural and Spectro-Ellipsometric Analysis. *Thin Solid Films* **2011**, *519*, 5924–5932.
- (28) Lu, Y.; Liu, G. L.; Lee, L. P. High-Density Silver Nanoparticle Film with Temperature-Controllable Interparticle Spacing for a Tunable Surface Enhanced Raman Scattering Substrate. *Nano Lett.* **2005**, *5*, 5–9.
- (29) Kundu, B.; Kurland, N. E.; Bano, S.; Patra, C.; Engel, F. B.; Yadavalli, V. K.; Kundu, S. C. Silk Proteins for Biomedical Applications: Bioengineering Perspectives. *Prog. Polym. Sci.* **2014**, 39, 251–267.
- (30) Rockwood, D. N.; Preda, R. C.; Yücel, T.; Wang, X.; Lovett, M. L.; Kaplan, D. L. Materials Fabrication from Bombyx Mori Silk Fibroin. *Nat. Protoc.* **2011**, *6*, 1612–1631.
- (31) Mandal, B. B.; Kundu, S. C. Osteogenic and Adipogenic Differentiation of Rat Bone Marrow Cells on Non-Mulberry and Mulberry Silk Gland Fibroin 3D Scaffolds. *Biomaterials* **2009**, *30*, 5019–5030.
- (32) Kang, Z.; Wang, Y.; Xu, J.; Song, G.; Ding, M.; Zhao, H.; Wang, J. An RGD-Containing Peptide Derived from Wild Silkworm Silk Fibroin Promotes Cell Adhesion and Spreading. *Polymer* **2018**, *10*, 1193.
- (33) Purnomo, X.; Setyarini, P. H.; Sulistyaningsih, D. Degradation Behavior of Silk Fibroin Biomaterials A Review. *J. Eng. Sci. Technol. Rev.* **2019**, *12*, *67*–74.
- (34) Cao, Y.; Wang, B. Biodegradation of Silk Biomaterials. *Int. J. Mol. Sci.* **2009**, *10*, 1514–1524.
- (35) Laomeephol, C.; Guedes, M.; Ferreira, H.; Reis, R. L.; Kanokpanont, S.; Damrongsakkul, S.; Neves, N. M. Phospholipid-Induced Silk Fibroin Hydrogels and Their Potential as Cell Carriers for Tissue Regeneration. *J. Tissue Eng. Regen. Med.* **2020**, *14*, 160–172
- (36) Kaushik, S.; Thungon, P. D.; Goswami, P. Silk Fibroin: An Emerging Biocompatible Material for Application of Enzymes and Whole Cells in Bioelectronics and Bioanalytical Sciences. *ACS Biomater. Sci. Eng.* **2020**, *6*, 4337–4355.
- (37) Kurland, N. E.; Dey, T.; Kundu, S. C.; Yadavalli, V. K. Precise Patterning of Silk Microstructures Using Photolithography. *Adv. Mater.* **2013**, 25, 6207–6212.
- (38) Pal, R. K.; Kurland, N. E.; Jiang, C.; Kundu, S. C.; Zhang, N.; Yadavalli, V. K. Fabrication of Precise Shape-Defined Particles of Silk Proteins Using Photolithography. *Eur. Polym. J.* **2016**, *85*, 421–430.
- (39) Kim, S. H.; Yeon, Y. K.; Lee, J. M.; Chao, J. R.; Lee, Y. J.; Seo, Y. B.; Sultan, M. T.; Lee, O. J.; Lee, J. S.; Yoon, S.; Hong, I.-S.; Khang, G.; Lee, S. J.; Yoo, J. J.; Park, C. H. Precisely Printable and Biocompatible Silk Fibroin Bioink for Digital Light Processing 3D Printing. *Nat. Commun.* **2018**, *9*, 1620.
- (40) Ju, J.; Hu, N.; Cairns, D. M.; Liu, H.; Timko, B. P. Photo-Cross-Linkable, Insulating Silk Fibroin for Bioelectronics with Enhanced Cell Affinity. *Proc. Natl. Acad. Sci.* **2020**, *117*, 15482–15489.

- (41) Abbas, M.; D'Amico, F.; Morresi, L.; Pinto, N.; Ficcadenti, M.; Natali, R.; Ottaviano, L.; Passacantando, M.; Cuccioloni, M.; Angeletti, M. Structural, Electrical, Electronic and Optical Properties of Melanin Films. *Eur. Phys. J. E: Soft Matter Biol. Phys.* **2009**, 28, 285–291.
- (42) Bothma, J. P.; de Boor, J.; Divakar, U.; Schwenn, P. E.; Meredith, P. Device-Quality Electrically Conducting Melanin Thin Films. *Adv. Mater.* **2008**, *20*, 3539.
- (43) Dezidério, S. N.; Brunello, C. A.; da Silva, M. I. N.; Cotta, M. A.; Graeff, C. F. O. Thin Films of Synthetic Melanin. *Proc. 20th Int. Conf. Amorph. Microcryst. Semicond.* **2004**, 338-340, 634–638.
- (44) Subianto, S.; Will, G.; Meredith, P. Electrochemical Synthesis of Melanin Free-Standing Films. *Polymer* **2005**, *46*, 11505–11509.
- (45) Roy, S.; Rhim, J.-W. Preparation of Carrageenan-Based Functional Nanocomposite Films Incorporated with Melanin Nanoparticles. *Colloids Surf., B* **2019**, *176*, 317–324.
- (46) Roy, S.; Rhim, J.-W. Agar-Based Antioxidant Composite Films Incorporated with Melanin Nanoparticles. *Food Hydrocolloids* **2019**, 94, 391–398.
- (47) Roy, S.; Van Hai, L.; Kim, H. C.; Zhai, L.; Kim, J. Preparation and Characterization of Synthetic Melanin-like Nanoparticles Reinforced Chitosan Nanocomposite Films. *Carbohydr. Polym.* **2020**, 231, 115729.
- (48) Xu, M.; Pradhan, S.; Agostinacchio, F.; Pal, R. K.; Greco, G.; Mazzolai, B.; Pugno, N. M.; Motta, A.; Yadavalli, V. K. Easy, Scalable, Robust, Micropatterned Silk Fibroin Cell Substrates. *Adv. Mater. Interfaces* **2019**, *6*, No. 1801822.
- (49) Muskovich, M.; Bettinger, C. J. Biomaterials-Based Electronics: Polymers and Interfaces for Biology and Medicine. *Adv. Healthcare Mater.* **2012**, *1*, 248–266.
- (50) Bradner, S. A.; Partlow, B. P.; Cebe, P.; Omenetto, F. G.; Kaplan, D. L. Fabrication of Elastomeric Silk Fibers. *Biopolymers* **2017**, *107*, No. e23030.
- (51) Noishiki, Y.; Nishiyama, Y.; Wada, M.; Kuga, S.; Magoshi, J. Mechanical Properties of Silk Fibroin-Microcrystalline Cellulose Composite Films. *J. Appl. Polym. Sci.* **2002**, *86*, 3425–3429.
- (52) Khan, S. P.; Auner, G. G.; Newaz, G. M. Influence of Nanoscale Surface Roughness on Neural Cell Attachment on Silicon. *Nanomed.: Nanotechnol., Biol. Med.* **2005**, *1*, 125–129.
- (53) Vahidzadeh, E.; Kalra, A. P.; Shankar, K. Melanin-Based Electronics: From Proton Conductors to Photovoltaics and Beyond. *Biosens. Bioelectron.* **2018**, *122*, 127–139.
- (54) Gidanian, S.; Farmer, P. J. Redox Behavior of Melanins: Direct Electrochemistry of Dihydroxyindole-Melanin and Its Cu and Zn Adducts. *J. Inorg. Biochem.* **2002**, *89*, 54–60.
- (55) Hong, L.; Simon, J. D. Insight into the Binding of Divalent Cations to Sepia Eumelanin from IR Absorption Spectroscopy. *Photochem. Photobiol.* **2006**, 82, 1265–1269.
- (56) Ligonzo, T.; Ambrico, M.; Augelli, V.; Perna, G.; Schiavulli, L.; Tamma, M. A.; Biagi, P. F.; Minafra, A.; Capozzi, V. Electrical and Optical Properties of Natural and Synthetic Melanin Biopolymer. *J. Non-Cryst. Solids* **2009**, 355, 1221–1226.
- (57) Ambrico, M.; Ambrico, P. F.; Cardone, A.; Ligonzo, T.; Cicco, S. R.; Di Mundo, R.; Augelli, V.; Farinola, G. M. Melanin Layer on Silicon: An Attractive Structure for a Possible Exploitation in Bio-Polymer Based Metal—Insulator—Silicon Devices. *Adv. Mater.* **2011**, 23, 3332—3336.
- (58) Jastrzebska, M. M.; Isotalo, H.; Paloheimo, J.; Stubb, H. Electrical Conductivity of Synthetic DOPA-Melanin Polymer for Different Hydration States and Temperatures. *J. Biomater. Sci. Polym. Ed.* **1996**, *7*, 577–586.
- (59) de Souza, F. S.; Costa, T. G.; Feldhaus, M. J.; Szpoganicz, B.; Spinelli, A. Nonenzymatic Amperometric Sensors for Hydrogen Peroxide Based on Melanin-Capped Fe 3+–, Cu 2+–, or Ni 2+– Modified Prussian Blue Nanoparticles. *IEEE Sens. J.* **2015**, *15*, 4749–4757.
- (60) da Silva, M. P.; Fernandes, J. C.; de Figueiredo, N. B.; Congiu, M.; Mulato, M.; de Oliveira Graeff, C. F. Melanin as an Active Layer in Biosensors. *AIP Adv.* **2014**, *4*, 37120.

I

- (61) Wu, T.-F.; Wee, B.-H.; Hong, J.-D. An Ultrasensitive and Fast Moisture Sensor Based on Self-Assembled Dopamine—Melanin Thin Films. *Adv. Mater. Interfaces* **2015**, 2, No. 1500203.
- (62) Kumar, P.; Di Mauro, E.; Zhang, S.; Pezzella, A.; Soavi, F.; Santato, C.; Cicoira, F. Melanin-Based Flexible Supercapacitors. *J. Mater. Chem. C* **2016**, *4*, 9516–9525.
- (63) Xu, R.; Gouda, A.; Caso, M. F.; Soavi, F.; Santato, C. Melanin: A Greener Route To Enhance Energy Storage under Solar Light. *ACS Omega* **2019**, *4*, 12244–12251.
- (64) Sheliakina, M.; Mostert, A. B.; Meredith, P. An All-Solid-State Biocompatible Ion-to-Electron Transducer for Bioelectronics. *Mater. Horiz.* **2018**, *5*, 256–263.
- (65) Green, R.; Abidian, M. R. Conducting Polymers for Neural Prosthetic and Neural Interface Applications. *Adv. Mater.* **2015**, 27, 7620–7637.
- (66) Cogan, S. F. Neural Stimulation and Recording Electrodes. *Annu. Rev. Biomed. Eng.* **2008**, *10*, 275–309.
- (67) Kim, Y. J.; Khetan, A.; Wu, W.; Chun, S.-E.; Viswanathan, V.; Whitacre, J. F.; Bettinger, C. J. Evidence of Porphyrin-Like Structures in Natural Melanin Pigments Using Electrochemical Fingerprinting. *Adv. Mater.* **2016**, *28*, 3173–3180.